


1S_0 hyperon superfluidity in neutron stars from a separable pairing force of finite rangeZhong-Hao Tu (涂中豪) ^{*}

CAS Key Laboratory of Theoretical Physics, Institute of Theoretical Physics, Chinese Academy of Sciences, Beijing 100190, China and School of Physical Sciences, University of Chinese Academy of Sciences, Beijing 100049, China



(Received 19 May 2022; accepted 10 August 2022; published 23 August 2022)

Starting from a separable pairing force of finite range of nucleons, a new set of the pairing strengths for the 1S_0 hyperon-hyperon pairing based on the quark model is proposed and the 1S_0 hyperon superfluidity in neutron stars with the new hyperon pairing strengths is investigated. The reliable $\Lambda\Lambda$ pairing strength is $2/3$ times NN pairing strength. The upper limit of $\Sigma\Sigma$ pairing strength is $2/3$ times NN pairing strength. The lower limit of the ratio of $\Xi\Xi$ pairing strength to NN pairing strength is 1. With these pairing strengths, the maximum $\Lambda\Lambda$ pairing gap is several tenths of a MeV which can be compared with the results calculated with the widely used pairing force ESC00; because of a low fraction of Σ^- hyperon, the Σ superfluidity is very weak or even absent in neutron stars; the Ξ superfluidity is stronger than the results calculated with ESC08c and the $\Xi^-\Xi^-$ pairing may potentially affect the cooling properties of massive neutron stars.

DOI: [10.1103/PhysRevC.106.025806](https://doi.org/10.1103/PhysRevC.106.025806)**I. INTRODUCTION**

The neutron star is one of the densest objects in our universe, and its central density can be several times the nuclear saturation density ρ_0 . Our knowledge of the interior of neutron stars, especially for the density region higher than $2\rho_0$, is uncertain yet. Hyperons could be populated in neutron-star cores and a number of works have been devoted to the study of neutron stars composed of hypernuclear matter; see, e.g., Refs. [1–11]. The appearance of hyperons results in two serious problems: One is the *hyperon puzzle*; i.e., hyperons strongly soften the equation of state (EOS) of neutron stars so that the maximum mass is not compatible with astrophysical observations [12–21]. The other one is that the hyperon direct Urca (dUrca) processes strongly enhance the neutrino luminosity and rapidly cool neutron stars [22–26] so that the surface temperatures of neutron stars are much lower than that observed [13,27,28]. For fixing the hyperon puzzle, several mechanisms that provide the additional repulsive interactions between baryons are introduced, see, e.g., Refs. [4,29–34], to increase the maximum mass of neutron stars; for the latter one, in order to weaken neutron-star cooling induced by hyperons, hyperons can be formed as a superfluid to suppress neutrino emission in the hyperon dUrca processes and to make the cooling curve of neutron stars compatible with the astrophysical observations.

Hyperons are paired at certain density regions in neutron-star cores [35–39]. The paired hyperons play an important role in neutron-star cooling [27]. On the one hand, the hyperon dUrca processes are exponentially suppressed by the hyperon superfluidity when $T \ll T_c$ [40–42], where T_c is the critical temperature of hyperon pairing. On the other hand, the hy-

peron pairing provides a new neutrino emission mechanism, i.e., the Cooper pair breaking and formation (PBF) mechanism [43]. This mechanism is also exponentially suppressed when $T_c \ll T$ but dominates the neutrino emissivities near the critical temperature [40,44]. The enhanced cooling paradigm resulting from any dUrca processes and the minimal cooling paradigm involving the PBF processes and the modified Urca processes have been proposed and they, including other scenarios, have been applied to studies of neutron-star cooling [45–59].

Hyperon superfluidity may potentially affect the glitches of pulsars. Glitches are the sudden changes of pulsars in their spin rate during the gradual and stable spin-down via electromagnetic radiation. The two-component model is a successful model to explain the occurrence of glitches [60,61]. In this model, the superfluid component in the inner crust of neutron stars is an angular momentum reservoir and it transfers angular momentum to the normal component when a glitch occurs. The inner crust is not enough to support a large glitch when the crustal entrainment in the crystal lattice is considered and therefore the two-component model falls into difficulty [62,63]; this is the so-called *glitch crisis*. There are two main ways that could give the two-component model a new life: One is to consider the effects of pairing of neutrons [64]; the other one is to include the superfluid component in neutron-star cores within the standard two-component model [65,66]. If the superfluid component is extended to the density range where the paired hyperons exist, the hyperon superfluidity takes effect in the two-component model. The possible contribution of the superfluid hyperons to the glitches may be supported by future research.

Our knowledge of the pairing gaps of hyperons, which determine the magnitudes of hyperon superfluidity, is uncertain so far. Focusing on 1S_0 hyperon-hyperon (YY) pairing, the pairing gap depends not only on YY pairing force but

^{*}tuzhonghao@mail.itp.ac.cn

also on the EOS of neutron stars. For $\Lambda\Lambda$ pairing, based on various $\Lambda\Lambda$ interactions, the maximum pairing gap at the Fermi surface (the pairing gaps I mention below are all at the Fermi surface) inside neutron stars may be 0.81 MeV (ESC00), $\sim 10^{-4}$ MeV (e.g., Urbana-type potential), or even absent (e.g., NSC97b) [67]. In several studies there is obtained the upper limit on the maximum pairing gaps of 0.55–1.10 MeV for $\Lambda\Lambda$ pairing and 1–3 MeV for $\Xi\Xi$ pairing [52,68]; the maximum pairing gaps for $\Sigma^-\Sigma^-$ pairing are about 8 MeV [38] and 3.5 MeV [69]. In this work, starting from the widely used separable pairing force of a finite range of nucleons, I will determine new pairing strengths for various YY pairings based on the quark model. The EOSs of neutron stars are calculated within the framework of the relativistic mean-field (RMF) model.

This paper is organized as follows. In Sec. II, the theoretical framework of the RMF model and the methodology for calculating EOSs of neutron stars are given. In Sec. III, I extend the pairing strength of nucleon to the hyperon sector,

and estimate the reliability of the pairing strengths for various YY pairings. In Sec. IV, I present the results and discussion on various YY pairing gaps in neutron stars and estimate the potential effects on the neutron-star cooling. Finally, a brief summary is given in Sec. V.

II. EQUATION OF STATE

The EOS relates the interior component to macroscopic properties (i.e., mass, radius, tidal deformability, etc.) of neutron stars. I assume that the nuclear matter inside neutron-star cores is composed of a β -equilibrated and charge-neutral mixture of nucleons (n and p), hyperons (Λ , $\Sigma^{\pm,0}$, and $\Xi^{0,-}$), and leptons (e^- and μ^-). The RMF model is used to calculate the EOSs of neutron stars. In this model, the baryons interact with each other through the exchange of isoscalar scalar and vector mesons (σ and ω), the isovector vector meson (ρ), and hidden-strangeness mesons (σ^* and ϕ). The Lagrangian density that describes the nuclear matter of neutron-star cores can be written as

$$\begin{aligned} \mathcal{L} = & \sum_B \bar{\psi}_B \{ \gamma^\mu [i\partial_\mu - g_{\omega B}\omega_\mu - g_{\rho B}\rho_\mu \boldsymbol{\tau}_B - g_{\phi B}\phi_\mu] - [M_B + g_{\sigma B}\sigma + g_{\sigma^* B}\sigma^*] \} \psi_B \\ & + \frac{1}{2} (\partial^\mu \sigma \partial_\mu \sigma - m_\sigma^2 \sigma^2) + \frac{1}{2} (\partial^\mu \sigma^* \partial_\mu \sigma^* - m_{\sigma^*}^2 \sigma^{*2}) - \frac{1}{4} W^{\mu\nu} W_{\mu\nu} + \frac{1}{2} m_\omega^2 \omega^\mu \omega_\mu \\ & - \frac{1}{4} \mathbf{R}^{\mu\nu} \mathbf{R}_{\mu\nu} + \frac{1}{2} m_\rho^2 \boldsymbol{\rho}^\mu \boldsymbol{\rho}_\mu - \frac{1}{4} \Phi^{\mu\nu} \Phi_{\mu\nu} + \frac{1}{2} m_\phi^2 \phi^\mu \phi_\mu + \sum_l \bar{\psi}_l (i\gamma_\mu \partial^\mu - m_l) \psi_l, \end{aligned} \quad (1)$$

where $\boldsymbol{\tau}_B$ are the Pauli matrices for isospin of the baryon species B ; M_B and m_l represent the baryon and lepton masses, respectively; $\psi_{B(l)}$ is the Dirac field of the baryon species B or the lepton species l ; σ , ω_μ , $\boldsymbol{\rho}_\mu$, σ^* , and ϕ_μ denote the quantum fields of mesons; and $W_{\mu\nu}$, $\mathbf{R}_{\mu\nu}$, and $\Phi_{\mu\nu}$ are the antisymmetric field strength tensors of the vector mesons ω , ρ , and ϕ , respectively. For the density-dependent (DD) RMF model, like DD-ME2 [70] and DD-MEX [71], the coupling constant between a baryon B and a meson m is density dependent and is parametrized by the relation $g_{mB}(\rho_B) = g_{mB}(\rho_0) f_m(\rho_B)$ with

$$\begin{aligned} f_m(\rho_B) &= a_m \frac{1 + b_m(\rho_B/\rho_0 + d_m)^2}{1 + c_m(\rho_B/\rho_0 + e_m)^2}, \quad m = \sigma \text{ and } \omega, \quad (2) \\ f_m(\rho_B) &= \exp[-a_m(\rho_B/\rho_0 - 1)], \quad m = \rho. \quad (3) \end{aligned}$$

For the nonlinear (NL) RMF model, like NL3 [72], all coupling constants are independent of the density, and the self-interaction term of the σ meson, $-g_2\sigma^3/3 - g_3\sigma^4/4$, is added in the Lagrangian density.

The relations of coupling constants between hyperons and vector mesons are given by the SU(6) quark model:

$$\begin{aligned} g_{\omega\Lambda} &= g_{\omega\Sigma} = 2g_{\omega\Xi} = \frac{2}{3}g_{\omega N}, \\ g_{\rho\Sigma} &= 2g_{\rho\Xi} = 2g_{\rho N}, \quad g_{\rho\Lambda} = 0, \quad (4) \\ 2g_{\phi\Lambda} &= 2g_{\phi\Sigma} = g_{\phi\Xi} = -\frac{2\sqrt{2}}{3}g_{\omega N}. \end{aligned}$$

As for the coupling constants between hyperons and scalar meson, the $g_{\sigma Y}$'s are determined by fitting the empirical hyperon potential $U_Y^{(N)}$ in symmetric nuclear matter at the saturation density:

$$U_Y^{(N)} = R_{\sigma Y} g_{\sigma N} \sigma^0 + R_{\omega Y} g_{\omega N} \omega^0 + \Sigma_R^0, \quad (5)$$

where R_{mY} is the ratio of g_{mY} to g_{mN} . Σ_R is the rearrangement term originating from the density dependence of the coupling constants between baryons and mesons and $\Sigma_R = 0$ for the NL-RMF model. σ^0 , ω^0 , and Σ_R^0 are the values of the corresponding meson fields and rearrangement term of the symmetric nuclear matter at the saturation density. I choose $U_\Lambda^{(N)} = -30$ MeV [67,73], $U_\Sigma^{(N)} = +30$ MeV, and $U_\Xi^{(N)} = -15$ MeV [67,74] in the present work. At the saturation density, the $g_{\sigma^* Y}$'s are obtained by fitting potential depths of hyperons in the hypernuclear matter:

$$U_Y^{(Y)} = g_{\sigma Y} \sigma^0 + g_{\omega Y} \omega^0 + g_{\sigma^* Y} \sigma^{*0} + g_{\phi Y} \phi^0 + \Sigma_R^0. \quad (6)$$

Here, I choose $U_\Xi^{(\Xi)} \simeq U_\Lambda^{(\Xi)} \simeq 2U_\Lambda^{(\Lambda)} \simeq 2U_\Xi^{(\Lambda)} \simeq -10$ MeV [75]. Because $U_Y^{(\Sigma)}$ is uncertain, one usually assumes $g_{\sigma^* \Lambda} = g_{\sigma^* \Sigma}$ [76,77]. In Table I, the coupling constants between hyperons and scalar mesons are listed.

Under the mean-field approximation, the meson fields are treated as classical fields. The equations of motion of various mesons are obtained via the Euler-Lagrange

TABLE I. Coupling constants between hyperons and scalar mesons and $R_s = (g_{\sigma Y}/g_{\sigma N})^2 + (g_{\sigma^* Y}/g_{\sigma N})^2$ for various hyperons with different effective interactions.

	$g_{\sigma\Lambda}/g_{\sigma N}$	$g_{\sigma\Sigma}/g_{\sigma N}$	$g_{\sigma\Xi}/g_{\sigma N}$	$g_{\sigma^*\Lambda(\Sigma)}/g_{\sigma N}$	$g_{\sigma^*\Xi}/g_{\sigma N}$	R_s^Λ	R_s^Σ	R_s^Ξ
DD-ME2	0.620035	0.470799	0.315064	0.479314	1.138528	0.614185	0.451394	1.395511
DD-MEX	0.617628	0.474792	0.311198	0.494965	1.147999	0.626455	0.470418	1.414746
NL3	0.618895	0.460889	0.309448	0.505989	1.158716	0.639056	0.468444	1.438381

equation

$$m_\sigma^2 \sigma = - \sum_B g_{\sigma B} \rho_B^v, \quad (7)$$

$$m_\omega^2 \omega = \sum_B g_{\omega B} \rho_B^v, \quad (8)$$

$$m_\rho^2 \rho = \sum_B g_{\rho B} \rho_B^v \tau_B^3, \quad (9)$$

$$m_{\sigma^*}^2 \sigma^* = - \sum_B g_{\sigma^* B} \rho_B^s \tau_B^3, \quad (10)$$

$$m_\phi^2 \phi = \sum_B g_{\phi B} \rho_B^v, \quad (11)$$

where τ_B^3 is the isospin projection of the baryon species B . The vector density ρ_B^v and scalar density ρ_B^s of the baryon species B read

$$\rho_B^v = \frac{(k_F^B)^3}{3\pi^2}, \quad (12)$$

$$\rho_B^s = \frac{1}{\pi^2} \int_0^{k_F^B} \frac{M_B^*}{\sqrt{k^2 + M_B^{*2}}} k^2 dk, \quad (13)$$

with the Fermi momentum k_F^B and effective mass $M_B^* = M_B + g_{\sigma B} \sigma + g_{\sigma^* B} \sigma^*$ of the baryon species B . The total baryon density ρ_B is written as $\rho_B = \sum_B \rho_B^v$. Inside neutron-star cores, the β -equilibrium condition and charge-neutral condition are fulfilled:

$$\mu_n - q_B \mu_e = \mu_B, \quad \mu_\mu = \mu_e, \quad (14)$$

$$\sum_B q_B \rho_B^v + \sum_l q_l \rho_l^v = 0, \quad (15)$$

where q_B is the charge of the baryon species B . $\mu_{B(l)}$ is the chemical potential of the baryon species B or lepton species l , and they are given by

$$\begin{aligned} \mu_B &= \sqrt{(k_F^B)^2 + M_B^{*2}} \\ &\quad + g_{\omega B} \omega + g_{\rho B} \rho \tau_B^3 + g_{\phi B} \phi + \Sigma_R, \\ \mu_l &= \sqrt{(k_F^l)^2 + M_l^{*2}}. \end{aligned} \quad (16)$$

The EOS, which is the pressure P as a function of the energy density ε , is calculated by solving the coupled Eqs. (7)–(11) and (14)–(15) at a given density region. The EOS and hyperon properties (e.g., the effective mass and Fermi momentum of the hyperon species Y) in neutron-star cores are crucial in determining the onset and strength of hyperon superfluidity. Taking the calculated EOS of the core and given EOS of the

crust as input, the mass-radius (M - R) relation of a stationary neutron star is obtained by solving the Tolman-Oppenheimer-Volkoff (TOV) equation [78,79]

$$\frac{dP}{dr} = - \frac{[P(r) + \varepsilon(r)][M(r) + 4\pi r^3 P(r)]}{r[r - 2M(r)]},$$

$$\frac{dM}{dr} = 4\pi r^2 \varepsilon(r), \quad (17)$$

where r is the distance from the center. R and $M(R)$ are the neutron-star radius and gravitational mass, respectively.

III. PAIRING STRENGTH FOR HYPERON

Under the Bardeen-Cooper-Schrieffer (BCS) approximation, the 1S_0 pairing gap $\Delta_B(k)$ of the baryon species B at zero temperature, which determines the onset of superfluidity, is obtained by solving the gap equation [35,67,80]

$$\Delta_B(k) = - \frac{1}{4\pi^2} \int k'^2 dk' \frac{V_{BB}(k, k') \Delta_B(k')}{\sqrt{[E(k') - E(k_F^B)]^2 + \Delta_B^2(k')}}}, \quad (18)$$

where the single-particle energy $E_B(k)$ of the baryon species B and the potential matrix element $V_{BB}(k, k')$ of the baryon-baryon pairing interaction in the 1S_0 channel are two important inputs. The single-particle energy in the RMF model is given by

$$E_B(k) = \sqrt{k^2 + M_B^{*2}} + g_{\omega B} \omega + g_{\rho B} \rho \tau_B^3 + g_{\phi B} \phi + \Sigma_R. \quad (19)$$

For pairing interaction, many-body theories have shown that its irreducible vertex at the lowest order is the bare baryon-baryon interaction [81,82]. As an approximation, $V_{BB}(k, k')$ can be written as

$$\begin{aligned} V_{BB}(k, k') &= \langle k | V_{BB}(^1S_0) | k' \rangle \\ &= 4\pi \int r^2 dr j_0(kr) V_{BB}(r) j_0(k'r), \end{aligned} \quad (20)$$

where $j_0(kr) = \sin(kr)/(kr)$ is the zeroth-order spherical Bessel function and $V_{BB}(r)$ denotes the 1S_0 baryon-baryon interaction in coordinate space. The hyperon-hyperon interactions are very uncertain; several hyperon-hyperon potentials have been used to study the superfluidity properties of Λ [35,37,52,67,69], Σ [38,69], and Ξ [52] in nuclear matter and neutron stars.

Tian *et al.* [83] derived a finite-range separable pairing force by fitting the 1S_0 nucleon pairing gap calculated with Gogny force. For Gogny force D1 parametrization, the separable pairing force of the nucleon is $V_{NN}(k, k') = G_N p(k)p(k') = G_N e^{-a^2 k^2} e^{-a^2 k'^2}$ with the pairing strength

$G_N = 738 \text{ MeV fm}^3$ and the effective range $a = 0.636 \text{ fm}$. With the separable pairing force, the energy gap equation (18) is rewritten as

$$1 = -\frac{1}{4\pi^2} \int k^2 dk \frac{G_N p^2(k)}{\sqrt{[E(k) - E(k_N^F)]^2 + \Delta_0^2 p^2(k)}} \quad (21)$$

with the trivial solution $\Delta(k) = \Delta_0 p(k)$. The critical temperature T_c can be obtained through the weak-coupling approximation $T_c \simeq 0.57\Delta_F$ with $\Delta_F = \Delta_0 p(k_F)$ [27,35]. Combining with the separable pairing force of the nucleon and the naive quark model, the $\Lambda\Lambda$ pairing strength $G_\Lambda = 4G_N/9$ was proposed and was applied to the investigation of Λ hypernuclei [84]. The ratio of the strength G_Λ to G_N is obtained by counting the number $n_{u/d}$ of u/d quarks in a Λ hyperon. Because only u/d quarks involve the coupling of a non-strangeness meson to a baryon at the tree level, the relation holds: $g_{mY} = (n_{u/d}/3)g_{mN}$, where the number 3 comes from the fact that a baryon is composed of three quarks. The interaction strength resulting from exchanging mesons between two baryons B is proportional to g_{mB}^2 [84]. Since the pairing force is the residual of the two-body baryon-baryon interaction, the pairing force is also proportional to g_{mB}^2 . For the Λ hyperon, its number of u/d quarks is 2, $G_\Lambda/G_N = (g_{m\Lambda}/g_{mN})^2 = n_{u/d}^2/9 = 4/9$. Although the relation $G_Y/G_N = (n_{u/d})^2/9$ is so far only used to study the multistrangeness Λ hypernuclei, it is easy to extend this relation to study the YY pairing in nuclear matter and neutron stars. Similarly, the YY pairing strengths are $G_\Sigma = 4G_N/9$ for Σ and $G_\Xi = G_N/9$ for Ξ .

In Ref. [84], it was assumed that g_{mY}/g_{mN} are the same for all non-strangeness mesons, and the hidden-strangeness mesons (e.g., σ^* and ϕ) are not included. Here I extend this relation to the case with the hidden-strangeness mesons in the framework of the RMF model, and g_{mY}/g_{mN} for various mesons need not be the same to each other. I consider the non-strangeness meson (σ , ω) and the hidden-strangeness mesons (σ^* , ϕ), and ρ is not included in this work. I assume that all mesons which mediate different interactions are independent of each other and the cross terms between various mesons are not included in the Lagrangian density. The effective ranges for different mesons are uncertain and thus I assume that they are the same. The pairing strength G_B can be written by the sum of the contributions from different mesons:

$$G_B = \sum_m G_{B,m} = G_{B,\sigma} + G_{B,\omega} + G_{B,\sigma^*} + G_{B,\phi}. \quad (22)$$

The independence between different mesons ensures that the relation holds for every meson: $G_{Y,m} = (g_{mY}/g_{mN})^2 G_{N,m}$. Since σ^* and ϕ mesons do not couple to nucleons, the couplings of strangeness mesons are usually determined by $g_{\sigma^*Y}/g_{\sigma N}$ and $g_{\phi Y}/g_{\phi N}$. Hence G_{Y,σ^*} and $G_{Y,\phi}$ are related to $G_{N,\sigma}$ and $G_{N,\omega}$, respectively. The ratio of G_Y to G_N can be written as

$$\frac{G_Y}{G_N} = \frac{R_s G_{N,\sigma} + R_v G_{N,\omega}}{G_{N,\sigma} + G_{N,\omega}}, \quad (23)$$

where $R_s = (g_{\sigma Y}/g_{\sigma N})^2 + (g_{\sigma^* Y}/g_{\sigma N})^2$ and $R_v = (g_{\omega Y}/g_{\omega N})^2 + (g_{\phi Y}/g_{\phi N})^2$. The values from the SU(6)

quark model are applied to the coupling constants between vector mesons (ω and ϕ) and hyperons; see Eq. (4). If the couplings of scalar mesons are the same as those of vector mesons [85], the pairing strengths for YY pairing are obtained as $G_\Lambda = 2G_N/3$, $G_\Sigma = 2G_N/3$, and $G_\Xi = G_N$.

In practice, the couplings of scalar mesons are determined by fitting empirical hyperon potentials in the RMF model. The G_Y/G_N is adjusted by the mean-field approximation. Using Eq. (5) and combining $U_Y^{(N)}$ and $U_N^{(N)}$, one obtains

$$R_{\sigma Y} = \frac{g_{\sigma Y}}{g_{\sigma N}} \simeq \frac{U_Y^{(N)} + R_{\omega Y}(g_{\sigma N}\sigma^0 - U_N^{(N)})}{g_{\sigma N}\sigma^0}. \quad (24)$$

The potential depth of nucleons is about -70 MeV and the scalar potential is about -400 MeV ; $R_{Y\omega}$ are the values from the SU(6) quark model. With these values, $R_{\sigma Y} < 2/3$ when $U_Y^{(N)} \gtrsim -46 \text{ MeV}$ for Λ and Σ and $R_{\sigma\Xi} < 1/3$ when $U_\Xi^{(N)} \gtrsim -23 \text{ MeV}$. The Λ hyperon potential is about -30 MeV and the Σ hyperon potential is generally considered to be repulsive ($U_\Sigma^{(N)} > 0$) [67,73]. Recently, Harada and Hirabayashi suggested a Ξ -nucleus potential of $-17 \pm 6 \text{ MeV}$ in the ${}^9\text{Be}$ (K^-, K^+) reaction [86]. Hence one concludes that $g_{\sigma Y}/g_{\sigma N}$ are always smaller than $g_{\omega Y}/g_{\omega N}$ from the SU(6) quark model, and the deviation of $g_{\sigma Y}/g_{\sigma N}$ from $g_{\omega Y}/g_{\omega N}$ for Σ is significantly greater than those for Λ and Ξ . Using Eq. (6), $g_{\sigma^* Y}$ are determined by fitting potential depths $U_Y^{(Y)}$ in the hypernuclear matter. Using DD-ME2, DD-MEX, and NL3, one obtains $g_{\sigma^* \Lambda(\Sigma)}/g_{\sigma N} = 0.479314, 0.494965, \text{ and } 0.505989$ which do not deviate much from $g_{\phi \Lambda(\Sigma)}/g_{\phi N}$. The strong attractive potential $U_\Xi^{(\Xi)}$ leads to $g_{\sigma^* \Xi}/g_{\sigma N} = 1.138528, 1.147999, \text{ and } 1.158716$ for DD-ME2, DD-MEX, and NL3 which all are significantly greater than $g_{\phi \Xi}/g_{\phi N}$. Taking these coupling constants into Eq. (23), one finds that $R_s < R_v$ for Λ and Σ , and the derivation of R_s from R_v for Σ is obviously larger than that for Λ due to the repulsive Σ hyperon potential. For Ξ , R_s is significantly larger than R_v due to the strong attractive potential $U_\Xi^{(\Xi)}$. The values of R_s are listed in Table I. In addition, because $G_N < 0$, $-G_{N,\sigma} > G_{N,\omega}$, and $G_Y < 0$, the lower limits of R_s for Λ and Σ are obtained: $R_s > -R_v G_{N,\omega}/G_{N,\sigma}$. In conclusion, the upper limits of G_Λ/G_N and G_Σ/G_N are $2/3$ and the lower limit of G_Ξ/G_N is 1.

IV. RESULTS AND DISCUSSION

In this section, I investigate the 1S_0 YY pairings in neutron stars and determine the YY pairing gaps by using the single-particle energy obtained in Sec. II and the YY pairing strengths derived in Sec. III. I employ three successful effective interactions, i.e., DD-ME2, DD-MEX, and NL3, to calculate the EOSs and M - R relations of neutron stars in our present work. In Ref. [11], it has been shown that DD-ME2 and DD-MEX produce the two stiffest EOSs in the case without the σ^* meson and the most massive neutron stars ($\gtrsim 2 M_\odot$) composed of hypernuclear matter. In this work, the σ^* meson is included in calculations. In Fig. 1, I display the EOSs and M - R relations of neutron stars calculated with DD-ME2, DD-MEX, and NL3. From Fig. 1(a), at low energy density ($\lesssim 500 \text{ MeV fm}^{-3}$), there is little difference between the pressures calculated with DD-ME2 and DD-MEX, and

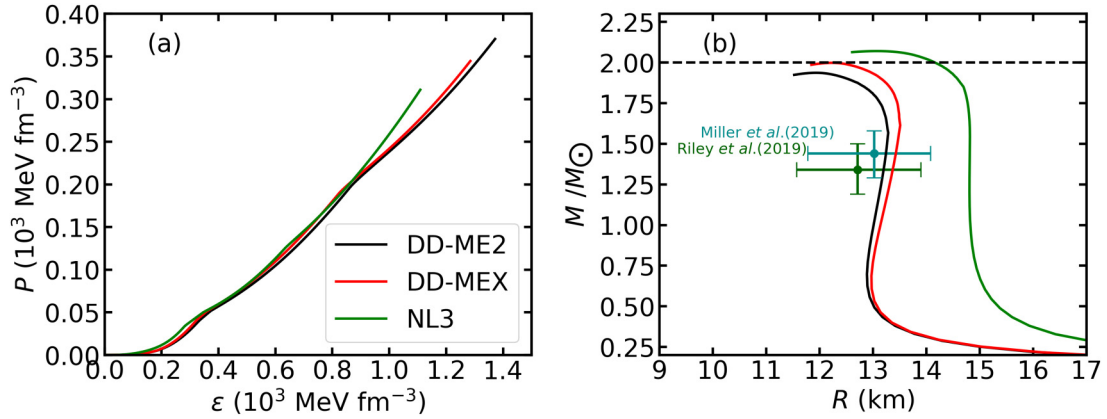


FIG. 1. (a) Equations of state and (b) mass-radius relations of neutron stars calculated with DD-ME2, DD-MEX, and NL3. In panel (b), the dashed line represents the constraint of $2 M_{\odot}$; the mass and radius of PSR J0030 + 0451 from NICER in Riley *et al.* [87] (dark green error bar) and Miller *et al.* [88] (dark cyan error bar) are also shown.

the EOS calculated with NL3 is slightly stiffer than the other two EOSs. At high energy density ($\gtrsim 800 \text{ MeV fm}^{-3}$), the EOS calculated with NL3 is significantly stiffer than those calculated with DD-ME2 and DD-MEX, and the stiffness of EOS calculated with DD-MEX is slightly larger than that calculated with DD-ME2.

Taking EOSs above as inputs, the corresponding M - R relations of neutron stars are calculated and are shown in Fig. 1(b). The BPS [89] and BBP [90] EOSs are chosen as the EOSs of the outer and inner crusts of neutron stars, respectively. The observed maximum mass of neutron stars is about $2 M_{\odot}$ [91–94]. The stiffnesses of EOSs at high density determine the theoretical maximum masses of neutrons stars. NL3 produces a maximum mass of about $2.07 M_{\odot}$ which is slightly larger than those calculated with DD-ME2 ($\sim 1.94 M_{\odot}$) and DD-MEX ($\sim 2.00 M_{\odot}$). Considering that the rotation of neutron stars can increase the maximum mass by about 20% [95–97], these EOSs I use in this work cannot be ruled out by the mass constraints from astrophysical observations. For the canonical neutron stars, the corresponding radii calculated with NL3 are significantly larger than those calculated with DD-ME2 and DD-MEX due to its stiffer EOS at low density. The radii calculated with NL3 are far away from the results from NICER [87,88], but this problem can be fixed by introducing a density-dependent isovector coupling [98].

With the single-particle energies of hyperons calculated with DD-ME2, DD-MEX, and NL3, the pairing gaps of various YY pairings as a function of the density are obtained by using the pairing strengths $G_Y = (n_{u/d}^2/9)G_N$, and the results are shown in Fig. 2. Because the effective ranges are assumed to be the same for all mesons, I use the YY pairing strength G_Y to represent the corresponding YY separable pairing force I mention below. For the Λ hyperon, the 1S_0 superfluid is formed as soon as the Λ hyperon is populated in neutron-star cores. The pairing gap increases with increasing density, then decreases after reaching a maximum pairing gap and finally vanishes at a higher density. One pays special attention to the maximum pairing gap which represents the strength of superfluidity. The maximum $\Lambda\Lambda$ pairing gaps are about 0.059 MeV, 0.057 MeV, and

0.051 MeV for DD-ME2, DD-MEX, and NL3. They are significantly smaller than the values widely used for calculations of neutron-star cooling [27,52,56,99] and the small pairing gap could cause the stronger hyperon dUrca process and the faster cooling of neutron stars. Among three effective interactions, only DD-MEX gives $\Sigma^- \Sigma^-$ pairing gaps with the maximum value 0.005 MeV. The corresponding critical temperature is about 10^7 K. The neutrino cooling, which dominates when the interior temperatures $T > 10^8$ K, lasts for 10^5 – 10^6 yr after the birth of neutron stars; thus the Σ superfluidity is absent before subsequent photon cooling [100]. The Ξ superfluidity vanishes in neutron-star cores due to the weak pairing strength $G_{\Xi} = (1/9)G_N$. The result is contrary to previous conclusions that Ξ hyperons are likely to form a superfluid and the pairing gaps of several MeV have been obtained [36,52]. The relation $G_Y = (n_{u/d}^2/9)G_N$ neglects the

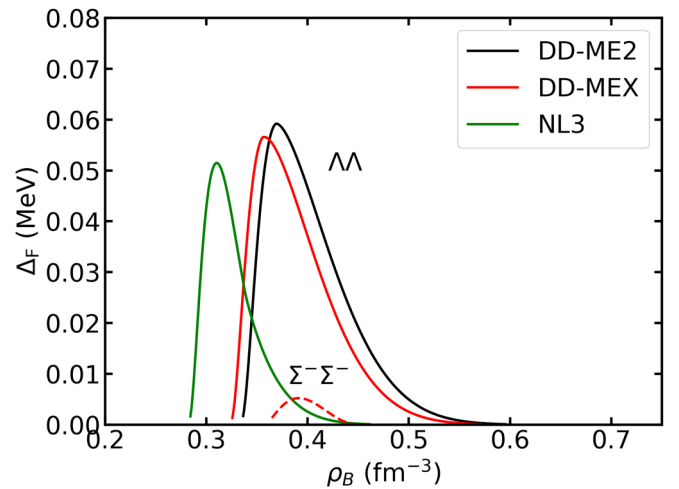


FIG. 2. 1S_0 pairing gaps of various YY pairings as a function of the density ρ_B in neutron stars with the pairing strengths $G_{\Lambda} = 4G_N/9$, $G_{\Sigma} = 4G_N/9$, and $G_{\Xi} = G_N/9$. The color lines represent results calculated with different effective interactions: DD-ME2 (black line), DD-MEX (red line), and NL3 (green line).

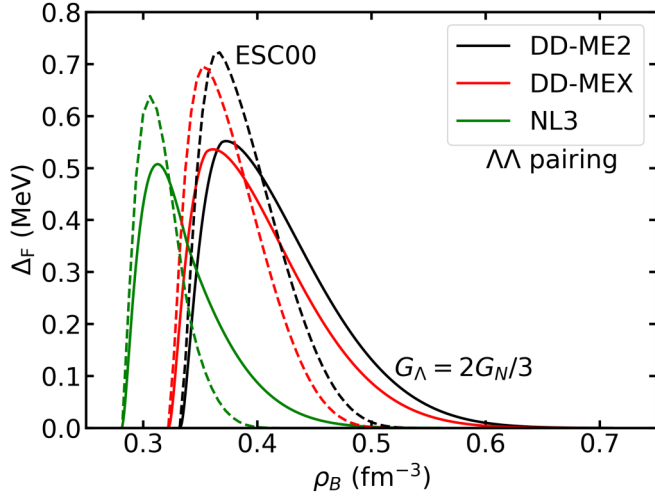


FIG. 3. 1S_0 $\Lambda\Lambda$ pairing gaps in neutron stars with $G_\Lambda = 2G_N/3$ (solid line) and ESC00 (dashed line). The color lines represent results calculated with different effective interactions: DD-ME2 (black line), DD-MEX (red line), and NL3 (green line).

contributions from the hidden-strangeness mesons (σ^* and ϕ) and leads to the weak YY pairing strengths, especially for Ξ hyperon with two s quarks.

Next, I calculate the 1S_0 pairing gaps of various YY pairings with $G_\Lambda = 2G_N/3$ for the $\Lambda\Lambda$ pairing, the upper limit of $\Sigma\Sigma$ pairing strength $G_\Sigma = 2G_N/3$, and the lower limit of $\Xi\Xi$ pairing strength $G_\Xi = G_N$. The contributions from σ^* and ϕ are included in the new pairing strengths.

A. $\Lambda\Lambda$ pairing

The pairing strength $G_\Lambda = 2G_N/3$ for $\Lambda\Lambda$ pairing is reliable because R_s is close to R_v . The resulting 1S_0 $\Lambda\Lambda$ pairing gaps in neutron stars are shown in Fig. 3. The phenomenological interaction ESC00 [101] is generally considered to provide maximum attraction in the $\Lambda\Lambda$ channel, and thus ESC00 maximizes the Λ superfluidity and generates the upper limit of the $\Lambda\Lambda$ pairing gap. The results calculated with ESC00 are also shown in Fig. 3 for comparison. The maximum pairing gaps calculated with $G_\Lambda = 2G_N/3$ are 0.552 MeV, 0.536 MeV, and 0.508 MeV for DD-ME2, DD-MEX, and NL3 and they are an order of magnitude larger than those calculated with $G_\Lambda = 4G_N/9$. The Λ superfluidity disappears at a larger density due to the larger $\Lambda\Lambda$ pairing gap. The ESC00 interaction still provides a maximum attraction so that

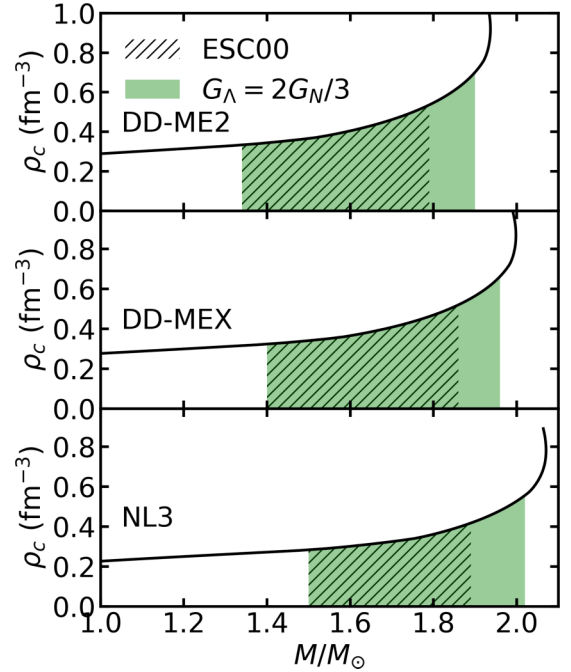


FIG. 4. Central density ρ_c as a function of neutron-star mass M for DD-ME2 (top), DD-MEX (middle), and NL3 (bottom). The mass regions where Λ hyperons form a 1S_0 superfluid are hatched ($G_\Lambda = 2G_N/3$) and shadows (ESC00), respectively.

the maximum pairing gaps calculated with it are larger than our results calculated with $G_\Lambda = 2G_N/3$. In Table II, I list the maximum 1S_0 $\Lambda\Lambda$ pairing gap (Δ_F^{\max}) and the corresponding density (ρ_B^{\max}), effective mass (M_B^*), and Fermi momentum (k_F^Λ) calculated with different pairing forces and effective interactions. Our results calculated with $G_\Lambda = 2G_N/3$ can be compared with those calculated with ESC00. Using a given pairing force, for various effective interactions, the larger Λ effective mass calculated with them, the larger the maximum pairing gap obtained.

Comparing with the pairing gaps calculated with ESC00, one notes that though the maximum pairing gaps calculated with $G_\Lambda = 2G_N/3$ are smaller, the Λ superfluidity can exist at higher densities where Λ hyperons are nonsuperfluid in the case of ESC00. In Fig. 4, I show the central density as a function of neutron-star mass and shade the mass regions where Λ hyperons form a 1S_0 superfluid. No matter which effective interaction is used, one finds that the Λ superfluidity

TABLE II. Maximum 1S_0 $\Lambda\Lambda$ pairing gap at the Fermi surface Δ_F^{\max} (in MeV) and the corresponding density ρ_B^{\max} (in fm^{-3}), effective mass M_B^* (in MeV), and Fermi momentum k_F^Λ (in fm^{-1}) calculated with different pairing forces and effective interactions.

	DD-ME2				DD-MEX				NL3			
	Δ_F^{\max} (MeV)	ρ_B^{\max} (fm^{-3})	M_B^* (MeV)	k_F^Λ (fm^{-1})	Δ_F^{\max} (MeV)	ρ_B^{\max} (fm^{-3})	M_B^* (MeV)	k_F^Λ (fm^{-1})	Δ_F^{\max} (MeV)	ρ_B^{\max} (fm^{-3})	M_B^* (MeV)	k_F^Λ (fm^{-1})
$2G_N/3$	0.552	0.373	716	0.843	0.536	0.362	710	0.841	0.508	0.313	698	0.849
$4G_N/9$	0.059	0.369	718	0.822	0.057	0.358	712	0.817	0.051	0.310	700	0.821
ESC00	0.722	0.367	719	0.801	0.695	0.352	716	0.768	0.638	0.306	704	0.770

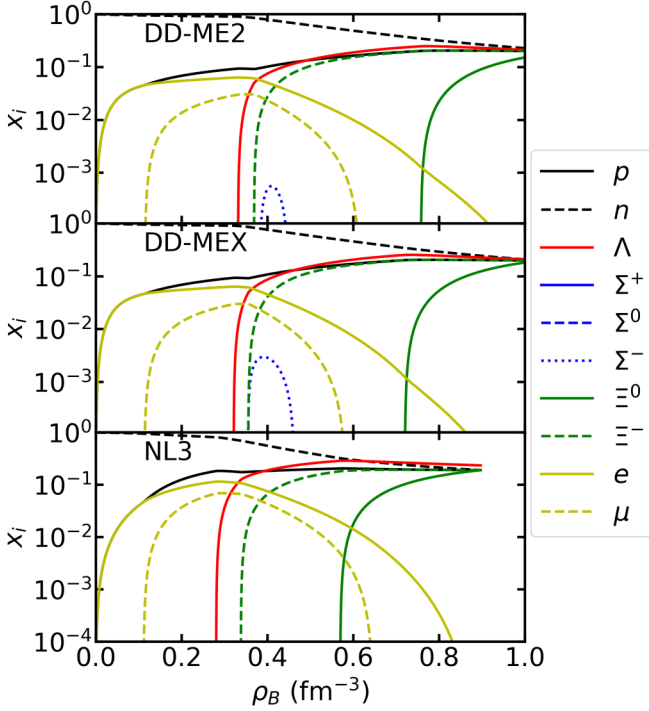


FIG. 5. Particle fraction X_i as a function of density ρ_B : DD-ME2 (top), DD-MEX (middle), and NL3 (bottom).

exists in neutron-star cores both for $G_\Lambda = 2G_N/3$ and ESC00. For all effective interactions, the mass regions only allowed for the existence of superfluid Λ hyperons with $G_\Lambda = 2G_N/3$ are wider than those with ESC00. The Λ superfluidity can exist in the central region of the heavier neutron stars; e.g., using DD-ME2, the upper limit of neutron-star mass that allows superfluid Λ hyperons to exist in the central region of a neutron star is $1.80 M_\odot$ for ESC00 and $1.90 M_\odot$ for $G_\Lambda = 2G_N/3$. Combining Figs. 3 and 4, for a massive neutron star, because $G_\Lambda = 2G_N/3$ produces a smaller $\Lambda\Lambda$ pairing gap compared with the case of ESC00, the hyperon dUrca process are stronger at low density, but at a higher density, the

pairing gap calculated with $G_\Lambda = 2G_N/3$ is larger and thus the hyperon dUrca process is weakened.

B. $\Sigma\Sigma$ pairing

The Σ superfluidity is calculated with the upper limit of $\Sigma\Sigma$ pairing strength $G_\Sigma = 2G_N/3$. Σ^0 and Σ^+ are charge-unfavored and thus they do not appear in our calculations. The presence and fraction of the Σ^- hyperon depend on the effective interaction. In Fig. 5, I show the particle fractions ($X_i = \rho_i^0/\rho_B$, $i = p, n, \Lambda, \Sigma^{\pm,0}, \Xi^{0,-}, e$, and μ^-) as a function of density ρ_B with DD-ME2, DD-MEX, and NL3. The Σ^- fractions are on the order of 10^{-4} and 10^{-3} for DD-ME2 and DD-MEX, respectively. The Σ^- hyperons are not populated in the calculation of NL3. The obtained maximum $\Sigma^-\Sigma^-$ pairing gaps are 0.008 MeV and 0.107 MeV which are significantly smaller than the results in Refs. [38,69]. The superfluid Σ^- hyperons do not exist in the core of a hot neutron star ($\gtrsim 10^9$ K). In fact, G_Σ/G_N could be significantly less than $2/3$ because of the large deviation between R_s^Σ and R_v^Σ . With the small Σ^- fractions, the strongest $\Sigma\Sigma$ pairing strength generates some small pairing gaps; one can draw the conclusion that the Σ superfluidity is very weak or even absent in neutron-star cores.

C. $\Xi\Xi$ pairing

The pairing strength $G_\Xi = G_N$ is the lower limit of $\Xi\Xi$ pairing strength as I discussed in Sec. III. Although G_Ξ/G_N may be much greater than 1, it is meaningful to find the magnitude of the maximum $\Xi\Xi$ pairing gap and estimate the influence of Ξ superfluidity on the cooling properties of neutron stars. The Ξ^- hyperon is charge-favored and thus its threshold density is smaller than that of Ξ^0 hyperon. The $\Xi\Xi$ pairing gaps calculated with $G_\Xi = G_N$ are shown in Fig. 6. For the case of NL3, the threshold density of the Ξ^0 hyperon is significantly smaller than those in the cases of DD-ME2 and DD-MEX. The reasons are as follows: On the one hand, the EOS calculated with NL3 is stiffer (see Fig. 1) and the Fermi energy of neutrons is larger so that the threshold condition

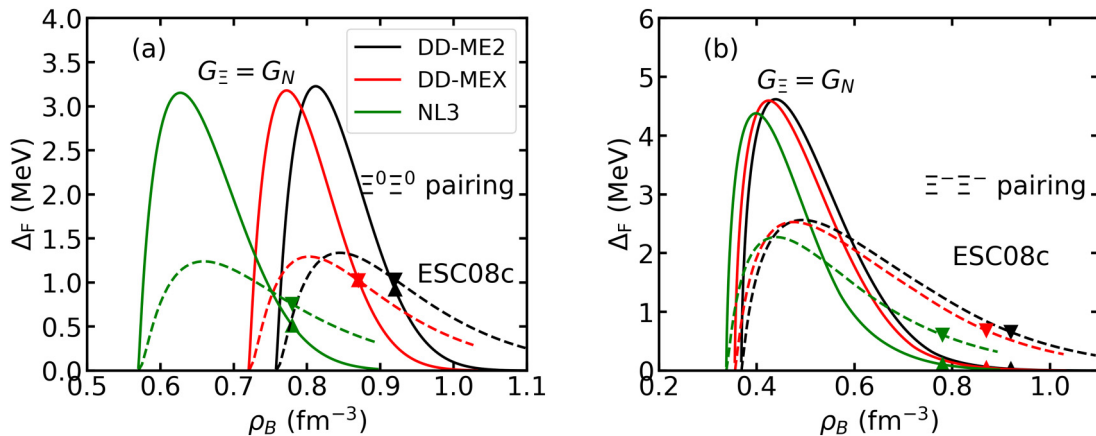


FIG. 6. 1S_0 pairing gaps of (a) $\Xi^0\Xi^0$ and (b) $\Xi^-\Xi^-$ in neutron stars with the pairing strength $G_\Lambda = G_N$ (solid line) and ESC08c (dashed line). The upper and lower triangles represent the pairing gaps in the central region of the most massive neutron star calculated with $G_\Lambda = G_N$ and ESC08c, respectively.

of Ξ^0 hyperon is easier to be fulfilled; on the other hand, the Fermi energy of the neutron is not suppressed by the populated Σ^- hyperons because they do not appear in the calculation of NL3. A $\Xi\Xi$ potential ESC08c has been applied to the investigations of neutron-star cooling [52,102]; the $\Xi\Xi$ pairing gaps calculated with ESC08c are also shown in Fig. 6.

From Figs. 6(a) and 6(b), using $G_{\Xi} = G_N$, the maximum pairing gaps are about 3.0–3.5 MeV for $\Xi^0\Xi^0$ pairing and 4–5 MeV for $\Xi^-\Xi^-$ pairing; they are significantly larger than the results calculated with ESC08c: 1.0–1.5 MeV for $\Xi^0\Xi^0$ pairing and 2–3 MeV for $\Xi^-\Xi^-$ pairing. Because $G_{\Xi}/G_N > 1$, the larger maximum $\Xi\Xi$ pairing gaps and the stronger Ξ superfluidity than previous results may exist in neutron-star cores [36,52]. One finds that the pairing gap calculated with $G_{\Xi} = G_N$ is larger than that calculated with ESC08c at low density but is smaller at high density. In the central region of the most massive neutron star, the pairing gaps calculated with $G_{\Xi} = G_N$ and ESC08c are on the order of 10^{-1} MeV and are compared for $\Xi^0\Xi^0$ pairing; for $\Xi^-\Xi^-$ pairing, the pairing gaps calculated with $G_{\Xi} = G_N$ are very small and those calculated with ESC08c are several tenths of a MeV. For $\Xi^-\Xi^-$ pairing, the large pairing gaps imply that dUrca processes involving Ξ^- hyperons are suppressed strongly inside neutron-star cores except in the central region of massive neutron stars. The neutron-star masses calculated with the threshold densities of Ξ^0 hyperon as the central densities are close to the top of M - R relations, i.e., $M(\rho_{\text{Thold}}^{\Xi^0} = 0.757 \text{ fm}^{-3}) = 1.92 M_{\odot}$ for DD-ME2, $M(\rho_{\text{Thold}}^{\Xi^0} = 0.720 \text{ fm}^{-3}) = 1.98 M_{\odot}$ for DD-MEX, and $M(\rho_{\text{Thold}}^{\Xi^0} = 0.570 \text{ fm}^{-3}) = 2.03 M_{\odot}$ for NL3; the Ξ^0 superfluidity only exists in the central region of massive neutron stars and hence Ξ^0 hyperons with a large pairing gap could hardly contribute to the cooling of neutron stars via the dUrca processes.

V. SUMMARY AND PERSPECTIVES

A new set of YY pairing strengths based on the quark model are proposed in this work. The contributions from every meson are considered to be independent of each other and the effective ranges induced by various mesons are assumed to be the same. The YY pairing strength G_Y can be written by the sum of the contributions from various mesons $G_{Y,m}$, and $G_{Y,m}$ is related to $G_{N,m}$ through the relation $G_{Y,m} = (g_{mY}/g_{mN})^2 G_{N,m}$. The SU(6) quark model and several empirical potentials are used to determine the ratios R_{Σ} and R_{Ξ} of the pairing strength of hyperons to that of nucleon. The reliable $\Lambda\Lambda$ pairing strength $G_{\Lambda} = 2G_N/3$, and the upper limit of $\Sigma\Sigma$ pairing strength $G_{\Sigma} = 2G_N/3$ and the lower limit of $\Xi\Xi$ pairing strength $G_{\Xi} = G_N$ are obtained. This set of

YY pairings strengths has included the contributions from hidden-strangeness mesons and has been applied to study the 1S_0 YY pairing in neutron-star cores.

The $\Lambda\Lambda$ pairing gaps calculated with $G_{\Lambda} = 2G_N/3$ are several tenths of a MeV and are compared with the results calculated with ESC00. The Λ superfluidity can exist in the central region of a massive neutron star. With the upper limit of $\Sigma\Sigma$ pairing strength $G_{\Sigma} = 2G_N/3$, the pairing gaps are small because of low fraction of Σ^- hyperon, and thus the Σ superfluidity is weak or even absent in neutron-star cores. With the lower limit of $\Xi\Xi$ pairing strength $G_{\Xi} = G_N$, both for Ξ^0 and Ξ^- hyperons, the pairing gaps are significantly larger than results calculated with ESC08c, implying that the Ξ superfluidity in neutron-star cores is stronger than that shown in Refs. [52,68]. Due to the large pairing gaps, the Ξ^- superfluidity strongly suppresses the corresponding dUrca processes inside neutron-star cores except in the central region of massive neutron stars; the Ξ^0 superfluidity could play a negligible role in the cooling of neutron stars.

Although the $\Lambda\Lambda$ pairing strength is reliable, the specific pairing strengths for Σ and Ξ hyperons are still very uncertain. The realistic values need to be fixed by further determining the exact contributions of σ and ω mesons to the effective pairing strength of the nucleon. The isospin effects of the hyperon pairing force should be considered and thus the ratios G_Y/G_N may be shifted, especially for the Σ hyperon. Besides, I also expect that the short and long corrections [103] on baryon-baryon pairing are included in future works. I expect that the new YY pairing strengths are useful not only to the investigations of nuclear matter and neutron-star matter, but also to the calculations of hypernuclei.

ACKNOWLEDGMENTS

Helpful discussions with Shan-Gui Zhou and Yu-Ting Rong are gratefully acknowledged. This work has been supported by the National Key R&D Program of China (Grant No. 2018YFA0404402), the National Natural Science Foundation of China (Grants No. 11525524, No. 12070131001, No. 12047503, and No. 11961141004), the Key Research Program of Frontier Sciences of the Chinese Academy of Sciences (Grant No. QYZDB-SSWSYS013), the Strategic Priority Research Program of the Chinese Academy of Sciences (Grants No. XDB34010000 and No. XDPB15), and the IAEA Coordinated Research Project (Grant No. F41033). The results described in this paper were obtained on the High-Performance Computing Cluster of ITP-CAS and the ScGrid of the Supercomputing Center, Computer Network Information Center of the Chinese Academy of Sciences.

- [1] N. K. Glendenning, *Astrophys. J.* **293**, 470 (1985).
- [2] J. Schaffner and I. N. Mishustin, *Phys. Rev. C* **53**, 1416 (1996).
- [3] A. Li, W. Zuo, A.-J. Mi, and G. Burgio, *Chin. Phys.* **16**, 1934 (2007).

- [4] S. Weissenborn, D. Chatterjee, and J. Schaffner-Bielich, *Phys. Rev. C* **85**, 065802 (2012).
- [5] M. Oertel, C. Providência, F. Gulminelli, and A. R. Raduta, *J. Phys. G: Nucl. Part. Phys.* **42**, 075202 (2015).
- [6] T. Katayama and K. Saito, *Phys. Lett. B* **747**, 43 (2015).

- [7] C. Providência, M. Fortin, H. Pais, and A. Rabhi, *Front. Astron. Space Sci.* **6**, 13 (2019).
- [8] B. Hong, Z.-Z. Ren, and D. Bai, *Commun. Theor. Phys.* **71**, 819 (2019).
- [9] V. B. Thapa, M. Sinha, J. J. Li, and A. Sedrakian, *Phys. Rev. D* **103**, 063004 (2021).
- [10] I. A. Rather, U. Rahaman, V. Dexheimer, A. A. Usmani, and S. K. Patra, *Astrophys. J.* **917**, 46 (2021).
- [11] Z.-H. Tu and S.-G. Zhou, *Astrophys. J.* **925**, 16 (2022).
- [12] H.-J. Schulze, A. Polls, A. Ramos, and I. Vidaña, *Phys. Rev. C* **73**, 058801 (2006).
- [13] Isaac Vidaña, *Nucl. Phys. A* **914**, 367 (2013).
- [14] T. Takatsuka, S. Nishizaki, and Y. Yamamoto, *Eur. Phys. J. A* **13**, 213 (2002).
- [15] D. Logoteta, I. Vidaña, and I. Bombaci, *Eur. Phys. J. A* **55**, 207 (2019).
- [16] D. Gerstung, N. Kaiser, and W. Weise, *Eur. Phys. J. A* **56**, 175 (2020).
- [17] Y. Yamamoto, T. Furumoto, N. Yasutake, and T. A. Rijken, *Phys. Rev. C* **88**, 022801(R) (2013).
- [18] Y. Yamamoto, T. Furumoto, N. Yasutake, and T. A. Rijken, *Phys. Rev. C* **90**, 045805 (2014).
- [19] T. Takatsuka, S. Nishizaki, and R. Tamagaki, *Prog. Theor. Phys. Suppl.* **174**, 80 (2008).
- [20] I. Vidaña, D. Logoteta, C. Providência, A. Polls, and I. Bombaci, *Europhys. Lett.* **94**, 11002 (2011).
- [21] S. Petschauer, J. Haidenbauer, N. Kaiser, U.-G. Meißner, and W. Weise, *Front. Phys.* **8**, 12 (2020).
- [22] M. Prakash, M. Prakash, J. M. Lattimer, and C. J. Pethick, *Astrophys. J.* **390**, L77 (1992).
- [23] C. J. Pethick, *Rev. Mod. Phys.* **64**, 1133 (1992).
- [24] P. Haensel and O. Y. Gnedin, *Astron. Astrophys.* **290**, 458 (1994).
- [25] M. Prakash, *Phys. Rep.* **242**, 297 (1994).
- [26] C.-R. Ji and D.-P. Min, *Phys. Rev. D* **57**, 5963 (1998).
- [27] C. Schaab, S. Balberg, and J. Schaffner-Bielich, *Astrophys. J.* **504**, L99 (1998).
- [28] Y. Xu, G.-Z. Liu, Y.-R. Wu, H.-Y. Wang, and F. Zhang, *Commun. Theor. Phys.* **56**, 521 (2011).
- [29] D. Lonardonì, A. Lovato, S. Gandolfi, and F. Pederiva, *Phys. Rev. Lett.* **114**, 092301 (2015).
- [30] R. Wirth and R. Roth, *Phys. Rev. Lett.* **117**, 182501 (2016).
- [31] S. Weissenborn, I. Sagert, G. Pagliara, M. Hempel, and J. Schaffner-Bielich, *Astrophys. J.* **740**, L14 (2011).
- [32] L. Bonanno and A. Sedrakian, *Astron. Astrophys.* **539**, A16 (2012).
- [33] T. Klähn, R. Łastowiecki, and D. Blaschke, *Phys. Rev. D* **88**, 085001 (2013).
- [34] K. Maslov, E. Kolomeitsev, and D. Voskresensky, *Phys. Lett. B* **748**, 369 (2015).
- [35] S. Balberg and N. Barnea, *Phys. Rev. C* **57**, 409 (1998).
- [36] T. Takatsuka, S. Nishizaki, Y. Yamamoto, and R. Tamagaki, *Prog. Theor. Phys.* **105**, 179 (2001).
- [37] T. Tanigawa, M. Matsuzaki, and S. Chiba, *Phys. Rev. C* **68**, 015801 (2003).
- [38] I. Vidaña and L. Tolós, *Phys. Rev. C* **70**, 028802 (2004).
- [39] X.-R. Zhou, H.-J. Schulze, F. Pan, and J. P. Draayer, *Phys. Rev. Lett.* **95**, 051101 (2005).
- [40] D. Yakovlev, A. Kaminker, O. Gnedin, and P. Haensel, *Phys. Rep.* **354**, 1 (2001).
- [41] D. Yakovlev and C. Pethick, *Annu. Rev. Astron. Astrophys.* **42**, 169 (2004).
- [42] D. Page and S. Reddy, *Annu. Rev. Nucl. Part. Sci.* **56**, 327 (2006).
- [43] E. Flowers, M. Ruderman, and P. Sutherland, *Astrophys. J.* **205**, 541 (1976).
- [44] L. Leinson and A. Pérez, *Phys. Lett. B* **638**, 114 (2006).
- [45] D. Page, J. M. Lattimer, M. Prakash, and A. W. Steiner, *Astrophys. J., Suppl. Ser.* **155**, 623 (2004).
- [46] D. Page, J. M. Lattimer, M. Prakash, and A. W. Steiner, *Astrophys. J.* **707**, 1131 (2009).
- [47] D. Page, M. Prakash, J. M. Lattimer, and A. W. Steiner, *Phys. Rev. Lett.* **106**, 081101 (2011).
- [48] W. G. Newton, K. Murphy, J. Hooker, and B.-A. Li, *Astrophys. J.* **779**, L4 (2013).
- [49] L. B. Leinson, *Phys. Lett. B* **741**, 87 (2015).
- [50] M. V. Beznogov, M. Fortin, P. Haensel, D. G. Yakovlev, and J. L. Zdunik, *Mon. Not. R. Astron. Soc.* **463**, 1307 (2016).
- [51] S. Han and A. W. Steiner, *Phys. Rev. C* **96**, 035802 (2017).
- [52] A. R. Raduta, A. Sedrakian, and F. Weber, *Mon. Not. R. Astron. Soc.* **475**, 4347 (2018).
- [53] S. Beloin, S. Han, A. W. Steiner, and D. Page, *Phys. Rev. C* **97**, 015804 (2018).
- [54] J. M. Dong, L. J. Wang, and W. Zuo, *Astrophys. J.* **862**, 67 (2018).
- [55] M. Fortin, G. Taranto, G. F. Burgio, P. Haensel, H.-J. Schulze, and J. L. Zdunik, *Mon. Not. R. Astron. Soc.* **475**, 5010 (2018).
- [56] A. R. Raduta, J. J. Li, A. Sedrakian, and F. Weber, *Mon. Not. R. Astron. Soc.* **487**, 2639 (2019).
- [57] A. Sedrakian, *Phys. Rev. D* **99**, 043011 (2019).
- [58] J.-B. Wei, G. F. Burgio, H.-J. Schulze, and D. Zappalà, *Mon. Not. R. Astron. Soc.* **498**, 344 (2020).
- [59] S. A. Bhat and A. Paul, *Eur. Phys. J. C* **80**, 544 (2020).
- [60] G. Baym, C. Pethick, D. Pines, and M. Ruderman, *Nature (London)* **224**, 872 (1969).
- [61] P. W. Anderson and N. Itoh, *Nature (London)* **256**, 25 (1975).
- [62] N. Andersson, K. Glampedakis, W. C. G. Ho, and C. M. Espinoza, *Phys. Rev. Lett.* **109**, 241103 (2012).
- [63] N. Chamel, *Phys. Rev. Lett.* **110**, 011101 (2013).
- [64] G. Watanabe and C. J. Pethick, *Phys. Rev. Lett.* **119**, 062701 (2017).
- [65] E. M. Kantor and M. E. Gusakov, *Astrophys. J.* **797**, L4 (2014).
- [66] A. Li, *Chin. Phys. Lett.* **32**, 079701 (2015).
- [67] Y. N. Wang and H. Shen, *Phys. Rev. C* **81**, 025801 (2010).
- [68] A. Sedrakian and J. W. Clark, *Eur. Phys. J. A* **55**, 167 (2019).
- [69] T. Takatsuka, S. Nishizaki, Y. Yamamoto, and R. Tamagaki, *Prog. Theor. Phys.* **115**, 355 (2006).
- [70] G. A. Lalazissis, T. Nikšić, D. Vretenar, and P. Ring, *Phys. Rev. C* **71**, 024312 (2005).
- [71] A. Taninah, S. Agbemava, A. Afanasjev, and P. Ring, *Phys. Lett. B* **800**, 135065 (2020).
- [72] G. A. Lalazissis, J. König, and P. Ring, *Phys. Rev. C* **55**, 540 (1997).
- [73] J. Schaffner-Bielich and A. Gal, *Phys. Rev. C* **62**, 034311 (2000).
- [74] C. Ishizuka, A. Ohnishi, K. Tsubakihara, K. Sumiyoshi, and S. Yamada, *J. Phys. G: Nucl. Part. Phys.* **35**, 085201 (2008).
- [75] J. Schaffner, C. Dover, A. Gal, C. Greiner, D. Millener, and H. Stocker, *Ann. Phys.* **235**, 35 (1994).
- [76] F. Yang and H. Shen, *Phys. Rev. C* **77**, 025801 (2008).

- [77] T. Miyatsu, M.-K. Cheoun, and K. Saito, *Phys. Rev. C* **88**, 015802 (2013).
- [78] R. C. Tolman, *Phys. Rev.* **55**, 364 (1939).
- [79] J. R. Oppenheimer and G. M. Volkoff, *Phys. Rev.* **55**, 374 (1939).
- [80] V. Khodel, V. Khodel, and J. Clark, *Nucl. Phys. A* **598**, 390 (1996).
- [81] E. M. Henley and L. Willets, *Phys. Rev.* **133**, B1118 (1964).
- [82] T. Duguet, *Phys. Rev. C* **69**, 054317 (2004).
- [83] Y. Tian, Z. Ma, and P. Ring, *Phys. Lett. B* **676**, 44 (2009).
- [84] Y.-T. Rong, P. Zhao, and S.-G. Zhou, *Phys. Lett. B* **807**, 135533 (2020).
- [85] H. Shen, *Phys. Rev. C* **65**, 035802 (2002).
- [86] T. Harada and Y. Hirabayashi, *Phys. Rev. C* **103**, 024605 (2021).
- [87] T. E. Riley, A. L. Watts, S. Bogdanov, P. S. Ray, R. M. Ludlam, S. Guillot, Z. Arzoumanian, C. L. Baker, A. V. Bilous, D. Chakrabarty, K. C. Gendreau, A. K. Harding, W. C. G. Ho, J. M. Lattimer, S. M. Morsink, and T. E. Strohmayer, *Astrophys. J.* **887**, L21 (2019).
- [88] M. C. Miller, F. K. Lamb, A. J. Dittmann, S. Bogdanov, Z. Arzoumanian, K. C. Gendreau, S. Guillot, A. K. Harding, W. C. G. Ho, J. M. Lattimer, R. M. Ludlam, S. Mahmoodifar, S. M. Morsink, P. S. Ray, T. E. Strohmayer, K. S. Wood, T. Enoto, R. Foster, T. Okajima, G. Prigozhin *et al.*, *Astrophys. J.* **887**, L24 (2019).
- [89] G. Baym, C. Pethick, and P. Sutherland, *Astrophys. J.* **170**, 299 (1971).
- [90] G. Baym, H. A. Bethe, and C. J. Pethick, *Nucl. Phys. A* **175**, 225 (1971).
- [91] P. B. Demorest, T. Pennucci, S. M. Ransom, M. S. E. Roberts, and J. W. T. Hessels, *Nature (London)* **467**, 1081 (2010).
- [92] J. Antoniadis, P. C. C. Freire, N. Wex, T. M. Tauris, R. S. Lynch, M. H. van Kerkwijk, M. Kramer, C. Bassa, V. S. Dhillon, T. Driebe, J. W. T. Hessels, V. M. Kaspi, V. I. Kondratiev, N. Langer, T. R. Marsh, M. A. McLaughlin, T. T. Pennucci, S. M. Ransom, I. H. Stairs, J. van Leeuwen *et al.*, *Science* **340**, 1233232 (2013).
- [93] H. T. Cromartie, E. Fonseca, S. M. Ransom, P. B. Demorest, Z. Arzoumanian, H. Blumer, P. R. Brook, M. E. DeCesar, T. Dolch, J. A. Ellis, R. D. Ferdman, E. C. Ferrara, N. Garver-Daniels, P. A. Gentile, M. L. Jones, M. T. Lam, D. R. Lorimer, R. S. Lynch, M. A. McLaughlin, C. Ng *et al.*, *Nat. Astron.* **4**, 72 (2020).
- [94] E. Fonseca, H. T. Cromartie, T. T. Pennucci, P. S. Ray, A. Y. Kirichenko, S. M. Ransom, P. B. Demorest, I. H. Stairs, Z. Arzoumanian, L. Guillemot, A. Parthasarathy, M. Kerr, I. Cognard, P. T. Baker, H. Blumer, P. R. Brook, M. DeCesar, T. Dolch, F. A. Dong, E. C. Ferrara *et al.*, *Astrophys. J., Lett.* **915**, L12 (2021).
- [95] F. Weber and N. K. Glendenning, *Astrophys. J.* **390**, 541 (1992).
- [96] G. B. Cook, S. L. Shapiro, and S. A. Teukolsky, *Astrophys. J.* **424**, 823 (1994).
- [97] V. Paschalidis and N. Stergioulas, *Living Rev. Relativity* **20**, 7 (2017).
- [98] X. Wu, S. Bao, H. Shen, and R. Xu, *Phys. Rev. C* **104**, 015802 (2021).
- [99] S. Tsuruta, J. Sadino, A. Kobelski, M. A. Teter, A. C. Liebmann, T. Takatsuka, K. Nomoto, and H. Umeda, *Astrophys. J.* **691**, 621 (2009).
- [100] D. Bandyopadhyay, S. Chakrabarty, P. Dey, and S. Pal, *Phys. Rev. D* **58**, 121301(R) (1998).
- [101] I. Filikhin and A. Gal, *Nucl. Phys. A* **707**, 491 (2002).
- [102] H. Garcilazo, A. Valcarce, and J. Vijande, *Phys. Rev. C* **94**, 024002 (2016).
- [103] D. Ding, A. Rios, H. Dussan, W. H. Dickhoff, S. J. Witte, A. Carbone, and A. Polls, *Phys. Rev. C* **94**, 025802 (2016).